

## Displacement current detection of photoconduction in carbon nanotubes

A. Mohite, S. Chakraborty, P. Gopinath, G. U. Sumanasekera, and B. W. Alphenaar<sup>a)</sup>  
*Department of Electrical and Computer Engineering and Department of Physics, University of Louisville,  
Louisville, Kentucky 40292*

(Received 6 May 2004; accepted 14 December 2004; published online 3 February 2005)

Using a capacitive photocurrent measurement technique, we demonstrate the ability of both semiconducting and metallic single wall nanotubes to function as photodetectors over a wide spectral range. We observe clear peaks in the photo induced displacement current of a nanotube-plated capacitor that correspond directly to the semiconducting and metallic transitions in the nanotube absorbance spectrum. The signal increases substantially as the carrier drift velocity is raised with applied bias. A large increase in the photocurrent observed below temperatures of 100 K suggests that the nanotube hot carrier relaxation rate decreases substantially at low temperatures. © 2005 American Institute of Physics. [DOI: 10.1063/1.1863447]

The potential for single wall carbon nanotubes (SWNTs) to function as optoelectronic device elements<sup>1</sup> was recognized soon after their discovery.<sup>2</sup> A SWNT behaves as a quasi-one-dimensional wire with an electron energy spectrum containing a series of sharp peaks known as van Hove singularities.<sup>3,4</sup> The energy spacing between van Hove singularities varies from less than 0.1 eV to more than 2 eV depending on the nanotube diameter. Optical excitation and recombination across pairs of van Hove peaks provides the possibility to create nanotube optical detectors or emitters that operate across a wide range of optical wavelengths.

A mat of SWNTs containing both semiconductor and metallic tubes shows three dominant photoabsorption peaks.<sup>5</sup> Kataura *et al.*<sup>6</sup> demonstrated that the three peaks correspond to the three primary transitions between pairs of van Hove singularities: the lowest energy semiconductor nanotube transition (S11), the next highest energy semiconductor nanotube transition (S22), and the lowest energy metallic nanotube transition (M11). Experiments have subsequently found that photoexcitation across pairs of van Hove peaks enhances the conductivity of semiconductor nanotubes, making nanotube photodetectors possible. Fujiwara *et al.*<sup>7</sup> measured the photocurrent of SWNT mats and observed peaks in the current corresponding to the S11 and S22 transitions. Following this work, the S22 peak was observed in photocurrent measurements of transistors made from individual SWNTs.<sup>8,9</sup>

There is only a small amount of published photocurrent data, and questions remain regarding the potential of SWNTs for photodetection applications. Despite the existence of higher energy SWNT optical transitions, results thus far have been limited to the infrared regime, in which both the S11 and S22 transitions lie. The photocurrent tends to drop off with increasing excitation energy, and little evidence for the M11 transition is observed. This creates a problem for SWNT detectors based on individual tubes, since successful device operation will depend on randomly selecting a semiconductor nanotube during fabrication.

Here, we present SWNT photocurrent measurements using a capacitive detection technique that demonstrate the ability of both metallic and semiconductor nanotubes to

function as photodetectors across a wide spectral range. In contrast to the standard photocurrent detection technique, we measure the photogenerated displacement current across a capacitor containing a nanotube mat electrode. This technique can provide higher signal to noise than standard photocurrent measurements since there is no dark current present. We have made a comparison of our results to absorbance data and find that the displacement current maps directly onto the nanotube electron energy spectrum. We are able to observe peaks corresponding to both semiconducting and metallic transitions in our spectrum, with no apparent decrease in sensitivity at increasing excitation energy. Using our technique, we also measure the temperature dependence of the photocurrent and observe a sharp increase in the photocurrent at low temperatures.

The SWNTs in our experiments are obtained from Carboxlex, Inc. Raman spectra using variety of excitation wavelengths exhibited radial breathing mode frequencies in the range 160–200  $\text{cm}^{-1}$  (Ref. 10) indicating the average tube diameters are roughly in the range 1.2–1.6 nm. This is consistent with TEM observations in which the most probable diameter is close to  $\sim 1.4$  nm (10,10 tubes). The sample is purified by oxidation in dry air for 30 min at 350 °C followed by reflux in 4 M HCl at  $T=120$  °C for 4 h. The purified sample is finally subjected to a vacuum degass at 1000 °C at  $10^{-7}$  Torr for 24 h. SWNT films are prepared by depositing ethanol-dispersed purified SWNT bundles onto a glass substrate under ambient conditions and then evaporating the ethanol at room temperature. The 300 K resistance of our nanotube films is measured to be approximately 10 ohm per square.

Our measurement set-up is shown in Fig. 1(a). A glass slide on which a SWNT film has been deposited is anchored to a copper block within an optical access flow cryostat. Contact to the SWNTs is made by attaching a gold wire to the corner of the film surface using silver paint. This allows the SWNT film and copper block to function as positive and negative electrodes of a capacitor, with the glass slide functioning as the capacitor dielectric. The device formed can be thought of as a metal-insulator-semiconductor (MIS) photodetector, except that the semiconductor is replaced by a SWNT mat.<sup>11</sup> The sample is illuminated using an optical parametric amplifier (OPA) excited by a pulsed Ti Sapphire regenerative amplifier. The pulse width is 120 fs with a rep-

<sup>a)</sup>Electronic mail: brucea@louisville.edu

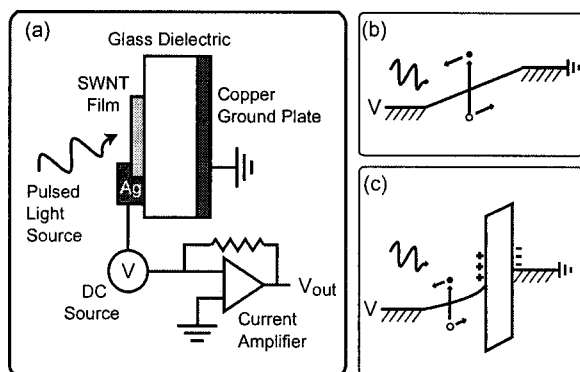


FIG. 1. (a) Diagram illustrating the displacement photocurrent measurement technique. The current is determined by measuring the output voltage using a lock-in amplifier set  $90^\circ$  out-of-phase from the pulsed laser repetition frequency. Electron energy diagrams are shown for (b) standard and (c) displacement photocurrent measurements (see text). Due to the absence of dark current, the displacement current technique is able to detect electron energy transitions in the metallic nanotubes.

etition rate of 1 kHz and the photon energy is tunable between 0.4 and 4 eV. The laser power was kept constant at 25 mW. Incident light focused onto the SWNT film optically generates 1 kHz ac displacement current across the capacitor, which is then amplified and measured using a lock-in detector.

Figure 2(a) shows the displacement current measured at 300 K as a function of photon energy for light directed at the SWNT film of a typical device. The displacement current varies as a function of photon energy with three peaks observed at 0.62, 1.39, and 1.85 eV. For comparison, we also measured the absorbance of the sampled by comparing the incident power to that transmitted through the nanotube mat. (A hole in the copper block allows for transmission measurements.) As shown in Fig. 2(b), peaks in the absorbance occur at the same energies at which peaks in the displacement

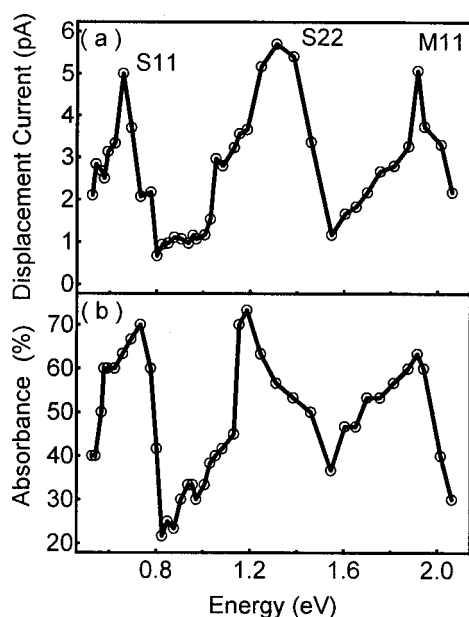


FIG. 2. (a) The displacement photocurrent of a SWNT film measured at 300 K as a function of incident photon energy. Peaks in the photocurrent are observed at the two lowest energy semiconductor transitions (S11 and S22) and at the lowest energy metallic transition (M11). (b) The absorbance measured for the same SWNT film under the same conditions.

current accurately probes the photoexcitation spectrum of the sample. Assuming an average nanotube diameter of 1.2 nm, the calculated energies for the three most prominent SWNT photoexcitation transitions are  $S11=0.65$  eV,  $S22=1.3$  eV, and  $M11=1.85$  eV.<sup>6</sup> As shown in Fig. 2, these match closely to the energies of the peaks observed in our displacement current spectrum, and an average diameter of 1.2 nm overlaps reasonably well with the predictions of Raman and TEM analysis.

There are two main differences between our results and those of Fujiwara *et al.* First, we observe a peak corresponding to the M11 transition, that was previously absent. Second, we observe that the photocurrent per photon increases with increasing photon energy, while previously, the opposite trend was observed. To understand these differences, we need to compare how photocurrent is generated in both the standard and displacement photocurrent techniques [illustrated in Figs. 1(b) and 1(c)]. In the standard photocurrent measurement [Fig. 1(b)], constant bias is applied across the SWNT film to produce a dark current that is dominated by transport through the metallic SWNTs. Optical excitation at either the S11 or S22 transition generates mobile carriers in the semiconductor SWNTs—this opens up a large number of new current pathways and produces an easily measurable photocurrent. Excitation at the M11 transition, on the other hand, results in a relatively small increase in current because no new current pathways are created and the metallic pathways do not become appreciably less resistive with the addition of optically excited carriers. In the displacement photocurrent measurement [Fig. 1(c)], the glass dielectric keeps the dark current at zero even under applied dc bias. A laser pulse incident on the SWNT mat excites mobile charge carriers, which redistribute to produce a temporary increase in the potential difference across the capacitor. For a 1 kHz repetition rate this results in a 1 kHz ac voltage across the capacitor and a measurable displacement current. Since this process can occur for carriers excited in either the semiconductor or metallic nanotubes, the M11, S11, and S22 transitions can all be observed.

The magnitude of the displacement current is determined by the number of optically excited electrons that travel from the SWNT mat and into the silver contact before energy relaxation occurs. In general, excited electrons will need to pass through a number of nanotube/nanotube junctions before reaching the silver contact. Since higher energy electrons are better able to overcome the potential barriers separating the SWNTs and the barrier into the contact, the displacement current per photon increases with increasing photon energy. We can also increase the displacement current by applying a positive dc bias to increase the electron drift velocity. This can be seen in the inset to Fig. 3(a) where the displacement current detected at the M11 transition is plotted as a function of bias on the silver contact. As the bias becomes more positive, the displacement current increases. The displacement current signal is still positive for zero bias, however, and continues to be positive even with negative bias on the contact.<sup>12</sup> This suggests that there is a built-in potential that aids in electron transfer away from the SWNT/glass interface and towards the silver contact. Such a potential can be created through the formation of a dipole layer at the nanotube/substrate interface due to interface states,<sup>13</sup> or due to work function differences between the nanotube and substrate.<sup>14</sup> Nanotube/substrate interface potentials as high as

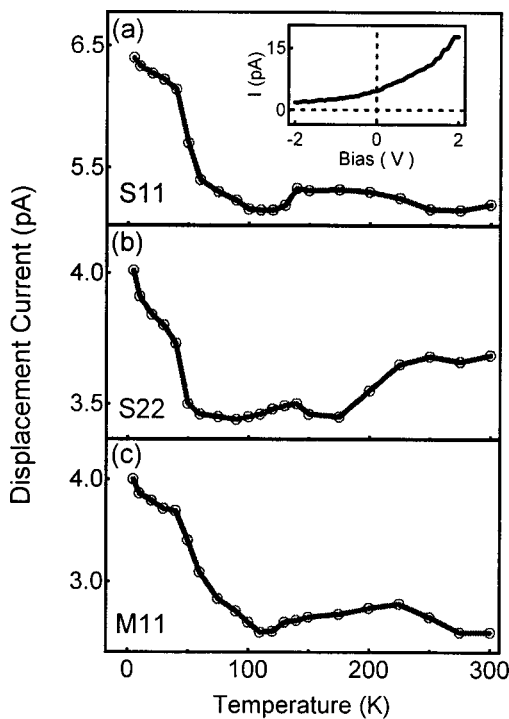


FIG. 3. Displacement photocurrent as a function of temperature for a second nanotube mat sample measured at the (a) S11, (b) S22, and (c) M11 transitions. Inset: The 300 K displacement photocurrent as a function of dc bias measured for the sample of Fig. 2 at the M11 transition.

0.17 V have been observed.<sup>13</sup> Recent experimental<sup>15</sup> and theoretical<sup>16</sup> work has shown that exciton binding energies in carbon nanotubes are extremely high, making excitons, rather than interband transitions, the primary photoexcitations in semiconducting SWNTs. The strong bias dependence in the photoconduction that we observe could thus also be due to the fact that bias aids in the separation of bound electron hole pairs.

Since the displacement current technique detects only those carriers that make it to the contact before energy relaxation occurs, the temperature dependence of the photocurrent provides a means to detect changes in the hot carrier relaxation rate as a function of temperature. In Fig. 3, the displacement current for excitation energies corresponding to the (a) S11, (b) S22, and (c) M11 transitions are shown as a function of temperature. (These are taken from measurements of a second SWNT mat sample.) In the 300–100 K range, the photocurrent is observed to either decrease or remain relatively constant. The exact temperature dependence in this range varies from sample to sample. Below 100 K, a

large increase in the photocurrent occurs that is observed in all samples and at all excitation energies measured. This increase implies that there is a decrease in the hot carrier recombination rate at low temperatures. The exact mechanism behind the decrease is still open to investigation, but it is thought to be due to the filling of trap based recombination centers at low temperature.

In conclusion, we have demonstrated the use of a displacement current technique to probe the photo excitation spectrum of a SWNT film. We observe a photocurrent signal corresponding to both semiconductor and metallic transitions with a large signal to noise ratio. This technique should also be generally applicable to individual nanotube and nanowire devices.

The authors thank S.Y. Wu, R.W. Cohn, J. Kielkopf, and P.C. Eklund for useful discussions. Funding provided by NSF (No. ECS-0224114) and NASA (No. NCC 5-571).

<sup>1</sup>Carbon Nanotubes: Synthesis, Structure, Properties and Applications, edited by M. Dresselhaus, G. Dresselhaus, and Ph. Avouris (Springer, Berlin, 2001).

<sup>2</sup>S. Iijima and T. Ichigashi, Nature (London) **363**, 603 (1993).

<sup>3</sup>N. Hamada, S. Sawada, and A. Oshiyama, Phys. Rev. Lett. **68**, 1579 (1992).

<sup>4</sup>R. Saito, M. Fujita, G. Dresselhaus, and M. S. Dresselhaus, Appl. Phys. Lett. **60**, 2204 (1992).

<sup>5</sup>M. E. Itkis, S. Niyogi, M. E. Meng, M. A. Hamon, H. Hu, and R. C. Haddon, Nano Lett. **2**, 155 (2002).

<sup>6</sup>H. Kataura, Y. Kumazawa, Y. Maniwa, I. Umezū, S. Suzuki, Y. Ohtsuka, and Y. Achiba, Synth. Met. **103**, 2555 (1999).

<sup>7</sup>A. Fujiwara, Y. Matsuoka, H. Suematsu, N. Ogawa, K. Miyano, H. Kataura, Y. Maniwa, S. Suzuki, and Y. Achiba, Jpn. J. Appl. Phys., Part 1 **40**, L1229 (2001).

<sup>8</sup>M. Freitag, Y. Martin, J. A. Misewich, R. Martel, and Ph. Avouris, Nano Lett. **3**, 1067 (2003).

<sup>9</sup>K. Balasubramanian, Y. Fan, M. Burghard, K. Kern, M. Friedrich, U. Wannek, and A. Mews, Appl. Phys. Lett. **84**, 2400 (2004).

<sup>10</sup>A. M. Rao, E. Richter, S. Bandow, B. Chase, P. C. Eklund, K. A. Williams, S. Fang, K. R. Subbaswamy, M. Menon, A. Thess, R. E. Smalley, G. Dresselhaus, and M. S. Dresselhaus, Science **275**, 187 (1997).

<sup>11</sup>A. Sher, R. K. Crouch, S. S.-M. Lu, W. E. Miller, and J. A. Moriarty, Appl. Phys. Lett. **32**, 713 (1978); A. Sher, Y. H. Tsuo, J. A. Moriarty, W. E. Miller, and R. K. Crouch, J. Appl. Phys. **51**, 2137 (1980).

<sup>12</sup>We note that the sign of the reverse bias signal, and the phase required to maximize the signal, varies from sample to sample. In some cases, a negative signal is observed at reverse bias, although in all cases the photoexcited IV characteristic is asymmetric with bias. These variations can be attributed to changes in the nanotube/substrate interface conditions.

<sup>13</sup>R. Czerw, B. Foley, D. Tekleab, A. Rubio, P. M. Ajayan, and D. L. Carroll, Phys. Rev. B **66**, 033408 (2002).

<sup>14</sup>A. G. Petrov and S. V. Rotkin, Nano Lett. **3**, 701 (2003).

<sup>15</sup>O. J. Korovyanko, C.-X. Sheng, Z. V. Vardeny, A. B. Dalton, and R. H. Baughman, Phys. Rev. Lett. **92**, 017403 (2004).

<sup>16</sup>C. D. Spataru, S. Ismail-Beigi, L. X. Benedict, and S. G. Louie, Phys. Rev. Lett. **92**, 077402 (2004).